光学学报

非线性光学超构表面：基础与应用

唐宇涛，张学才，胡子贤，胡悦，刘萱，李贵新*

南方科技大学工学院材料科学与工程系，广东 深圳 518055

摘要 光学超构表面是一种由亚波长尺度的超构单元在面内排布而构成的准二维人工结构材料。研究人员可以通过选择超构单元的材料组成、几何形状对光的振幅、偏振、相位和频率等光场自由度进行灵活调控。聚焦于超构表面在非线性光场调控领域的原理与应用。首先，概述了非线性晶体到非线性超构表面的发展历程。然后，讨论了对称性和几何相位在非线性光学超构表面中的重要作用。最后，介绍了非线性光学超构表面在波前调控、量子信息处理和太赫兹波的产生与调控等领域中的应用。

关键词 光学设计；非线性光学；光学超构表面；波前调控

中图分类号 O436 **文献标志码** A **DOI：** 10.3788/AOS230428

1 引 言

非线性光学在光与物质相互作用的研究中起着重要的作用，是现代光学研究的重要分支。材料的非线性光学响应能用于材料性质的表征，非线性光学频率转换、光折变等也被广泛应用于激光光源、光信息处理等领域中[1]。激光的发明极大地促进了非线性光学的发展。非线性光学效应与入射激光的电场、材料的非线性极化率和相位匹配等因素密切相关。在严格的相位匹配条件难以实现的情况下，利用晶体中非线性极化率的空间调制对波矢失配进行补偿的准相位匹配技术可有效提高非线性转换效率。近年来，随着非线性光学器件朝着微型化、集成化和多功能化方向发展，对非线性光场进行多维度调控逐渐成为重要的研究方向。光学超构表面的出现有望在这一领域中发挥重要作用。作为一种由亚波长尺度的超构单元组成的人工结构材料，超构表面具有光学损耗小、加工制备简单等优点。超构表面结构单元的材料和形状可以根据不同的物理机制进行选择，它们在二维平面内的排布方式也可以根据不同的应用场景进行工程化设计，为发展新型多功能光学器件提供了极大的自由度。

通过合适的材料选择和超构单元设计，光学超构表面可以用于调控非线性光学过程。得益于超构表面的超薄特性，相位匹配条件不像在传统晶体中那样重要。然而，组分材料和超构单元及其排布的对称性往往会决定超构表面器件的非线性光学响应特性。通过合理的对称性设计，并利用共振、几何相位等原理，超构表面能够在产生非线性光场的同时，对其振幅、相位、偏振和波前等参量进行调控。本文综述了近年来非线性光学超构表面的研究进展。首先，概述了传统晶体到非线性光学超构表面的发展历程。然后，讨论了非线性光学超构表面的设计原理。最后，介绍了非线性光学超构表面在波前调控、量子信息处理，以及太赫兹波的产生与调控等领域中的应用。

2 从传统晶体到非线性光学超构表面

2.1 双折射晶体相位匹配

1961 年，Franken 等[2]将波长为 694.3 nm 的聚焦激光束入射到石英晶体内，观察到了波长为 347.2 nm 的二次谐波信号，由此揭开了非线性光学的全新篇章[3]。在偶极近似下，材料对光场的响应可以用极化强度 P 表示，$P=\varepsilon_0[\chi^{(1)}E+\chi^{(2)}E^2+\chi^{(3)}E^3+\cdots]$，其中 ε_0 为真空介电常数，E 为入射光的电场，$\chi^{(1)}$ 为材料的线性极化率，$\chi^{(2)}$ 和 $\chi^{(3)}$ 分别为材料的二阶和三阶非线性极化率[4-5]。在线性光学中，$\chi^{(2)}$ 等高阶非线性极化率可以忽略，P 和 E 成正比，出射光场的频率和入射光场相同。当入射光的电场 E 很强时，材料对光场的高阶非线性响应不能被忽略，故会引发许多奇妙的物理过程，如基于二阶非线性光学响应的倍频（SHG）、和频（SFG）和差频（DFG）效应，以及基于三阶非线性光学响应的三倍频（THG）和四波混频（FWM）效应等。

在 1962 年为非线性光学奠定理论基础的文章中，Armstrong 等[6]指出动量守恒条件对于提高非线性光

收稿日期：2023-01-02；**修回日期**：2023-02-03；**录用日期**：2023-02-10；**网络首发日期**：2023-02-20

基金项目：国家自然科学基金（91950114，12161141010）

通信作者：*ligx@sustech.edu.cn

学转换效率是至关重要的。以倍频过程为例，当基频光波矢 $\boldsymbol{k}_1$ 和倍频光波矢 $\boldsymbol{k}_2$ 不满足动量守恒条件时，即存在波矢失配 $\Delta\boldsymbol{k}=\boldsymbol{k}_2-2\boldsymbol{k}_1$，倍频光的振幅每经过一段相干距离 $L_c=\pi/|\Delta\boldsymbol{k}|$ 的累积增长就会转至降低状态，这使得倍频光的能量周期性振荡，振荡周期为 $2L_c$。因此，理想的非线性转换效率要求波矢匹配条件为 $\Delta\boldsymbol{k}=0$。

一种实现严格相位匹配的方法是利用晶体的双折射效应。在双折射晶体中，寻常光（o光）和非寻常光（e光）的偏振方向互相垂直且二者折射率不同。在特定角度入射的条件下，o光和e光的折射率差异使得基频光和非线性光实现严格的相位匹配，从而可以提高非线性转换效率。这种方法最初由 Giordmaine[7] 和 Maker 等[8] 分别于 1962 年独立基于实验提出，他们使用的晶体均为磷酸二氢钾（KDP）晶体。1965 年，Midwinter 等[9] 针对二阶非线性光学过程总结出了两类相位匹配的方式，第一类相位匹配方式中基频光的偏振方向相同（均为o光或e光），第二类相位匹配方式中基频光的偏振方向正交（一束基频光为o光，另一束基频光为e光）。对于和频过程（$\omega_3=\omega_1+\omega_2$），在正单轴晶体和负单轴晶体中，两类相位匹配条件要求的折射率和频率关系如表1所示。其中，n_1、n_2 和 n_3 为对应于频率为 ω_1、ω_2 和 ω_3 的折射率，其上标o或e表示该频率的光取o光或e光的偏振方向。

表1　单轴晶体实现和频过程（$\omega_3=\omega_1+\omega_2$）的相位匹配条件[5]

Table 1　Phase-matching conditions for realizing sum frequency generation ($\omega_3=\omega_1+\omega_2$) in uniaxial crystals[5]

Type	Positive uniaxial ($n_e>n_o$)	Negative uniaxial ($n_e<n_o$)
I	$n_3^o\omega_3=n_1^e\omega_1+n_2^e\omega_2$	$n_3^e\omega_3=n_1^o\omega_1+n_2^o\omega_2$
II	$n_3^o\omega_3=n_1^o\omega_1+n_2^e\omega_2$	$n_3^e\omega_3=n_1^e\omega_1+n_2^o\omega_2$

2.2　准相位匹配和非线性光子晶体

利用各向异性晶体进行严格的相位匹配可以有效地提高非线性光学转换效率，但有一定的局限性。例如，在某些频段很难找到合适的双折射晶体，从而很难实现严格的相位匹配。此时，可以通过在晶体中引入非线性极化率的空间调制使非线性光场的强度保持单调增长[6,10]，这实际上是在空间上对非线性极化率进行周期性调制。利用非线性极化率在傅里叶空间的倒格矢为非线性过程提供额外的动量补偿，达到动量匹配的效果，这一方法也被称为准相位匹配，如图1(a)所示，其中 ω 为泵浦光的频率，2ω 为产生的倍频光的频率，k_ω 和 $k_{2\omega}$ 为相应的波矢大小，Λ 为超晶格结构的周期，G_m 为傅里叶空间中的倒格矢大小。准相位匹配的最初设想是通过翻转晶体的晶轴实现的，但这涉及到对晶体进行相干长度量级上的切割，故实现起来非常困难[6]。在生长晶体的过程中直接改变晶体晶向的方法为实现准相位匹配提供了新的思路[11]。20 世纪 90 年代，人们发现可以通过加电改变铁电晶体的铁电畴朝向来实现非线性极化率的翻转，从而使得准相位匹配技术变得方便且可靠[12]。实验中通常采用的晶体有钽酸锂（$LiTaO_3$）晶体、铌酸锂（$LiNbO_3$, LN）晶体和磷酸钛氧钾（$KTiOPO_4$, KTP）晶体等[10]。

将传统准相位匹配技术中对二阶非线性极化率的周期性调制推广成准周期性调制就可以提供更丰富的动量补偿过程[13-14]。例如，按一维 Fibonacci 序列调制的准周期非线性光学超晶格可以对倍频过程和倍频光与基频光的和频过程同时进行动量补偿，使其均满足准相位匹配条件[14]，如图1(b)所示。因此，通过一块具有二阶非线性极化率的晶体就能同时实现倍频和三倍频的产生，且三倍频的转换效率高达23%。材料的

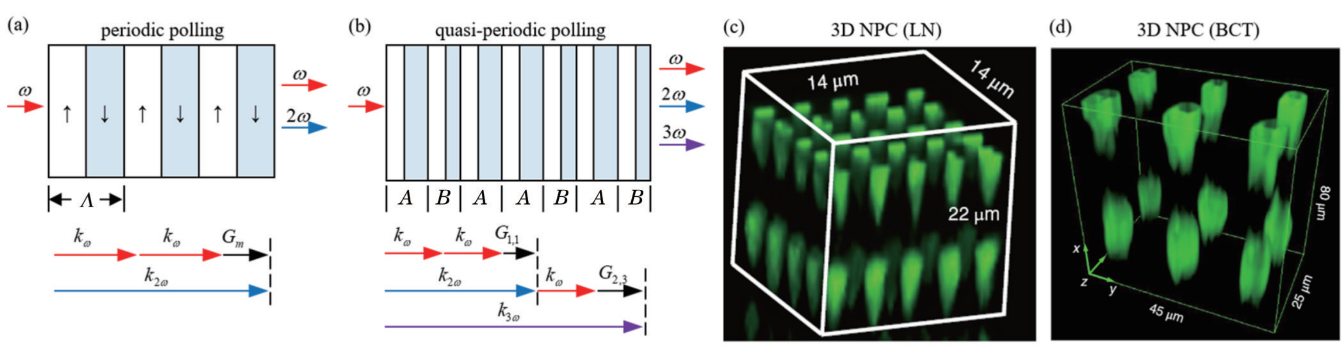

图1　准相位匹配技术和非线性光子晶体。(a)一维周期性极化非线性光子晶体产生倍频光的准相位匹配条件；(b)一维准周期极化非线性光子晶体产生倍频和三倍频光的准相位匹配条件[14]；(c)基于LN晶体的三维非线性光子晶体[19]；(d)基于BCT晶体的三维非线性光子晶体[20]

Fig. 1　Quasi-phase matching and nonlinear photonic crystals. (a) Quasi-phase matching conditions for second harmonic generation in one-dimensional periodic polarized nonlinear photonic crystal; (b) quasi-phase matching conditions for second harmonic generation and third harmonic generation in one-dimensional quasi-periodic polarized nonlinear photonic crystal[14]; (c) three-dimensional nonlinear photonic crystal fabricated in LN crystal[19]; (d) three-dimensional nonlinear photonic crystal fabricated in BCT crystal[20]

本征三阶非线性极化率较弱，这种准周期准相位匹配方法为高效产生三倍频提供了一种新的技术路径，并且可以推广至高阶非线性过程中[15-16]。

受准相位匹配技术和光子晶体概念的启发，Berger[17]于1998年提出了非线性光子晶体（NPC）的概念。通过准相位匹配技术实现高效非线性转化的同时，利用光子晶体的禁带特性等实现对非线性光场的调控，由此实现频谱和波前的多重调控。限于当时的制备技术，Berger提出的非线性光子晶体主要指对$\chi^{(2)}$进行一维和二维调制。2009年，Chen等[18]在理论上研究了三维非线性光子晶体中的相位匹配问题。2018年，Wei等[19]和Xu等[20]首次基于飞秒激光直写技术制备了三维非线性光子晶体，如图1(c)和图1(d)所示。他们分别使用透明的铌酸锂晶体和钛酸钡钙（BCT）晶体将飞秒激光聚焦至晶体的不同位置，对$\chi^{(2)}$进行“擦除”或“重定向”，并利用三维准相位匹配技术对所产生的倍频光场进行调控。在此基础上，他们也基于三维非线性光子晶体实现了对倍频光的波前调控[21-22]。近来，人们成功制备了可反复擦写、最小线宽可达30 nm的三维非线性光子晶体[23]。相关技术有望在非线性波前调控、非线性全息成像和多维纠缠光源等领域中发挥重要作用[24-25]。

2.3 非线性光学超构表面

在过去二十几年间，非线性光学超构材料和非线性光学超构表面领域的研究取得了重要进展。20世纪60年代，Veselago等[26]指出当介电常数ε和磁导率μ均为负数时，材料的折射率是负值，并预测了一系列新奇的光物理现象。2001年，Shelby等[27]首次从实验上在微波波段中实现了等效介电常数$\varepsilon_{\mathrm{eff}}$和等效磁导率$\mu_{\mathrm{eff}}$均小于零的负折射率材料。此后，通过在亚波长尺度上调控超构材料的ε和μ实现了超分辨成像、隐身衣等[28-31]。超构表面作为准二维的超构材料，相对于三维超构材料来说具有光学损耗小、易于制备等优点，有利于光学器件的小型化、集成化。在线性光学领域，研究人员通过对透射或反射光场的振幅、相位和偏振等自由度进行有效调控，实现了许多基于超构表面的微纳光学元件，如波片、平面透镜等[32-38]。

与此同时，超构表面也是提高非线性光学转化效率的重要材料体系[39-43]。例如，Pendry等[44]指出谐振环开口处的局域共振效应可用于实现拉曼信号的增强，如图2(a)所示。采用具有中心反演对称破缺的U形超构单元并引入局域等离激元共振（LSPR）可提高倍频光的产生效率[45]，如图2(b)所示。进一步引入纳米光腔设计可使得U形超构表面上的倍频效率提高两个数量级以上[46]。设计具有泵浦光和倍频光双共振特性的等离激元超构表面也可以提高倍频光的产生效率[47]，如图2(c)所示。此外，集体效应、晶格共振[48-50]和无源单元[51]等物理机制也被广泛用来提高等离激元超构表面的二阶非线性转换效率。

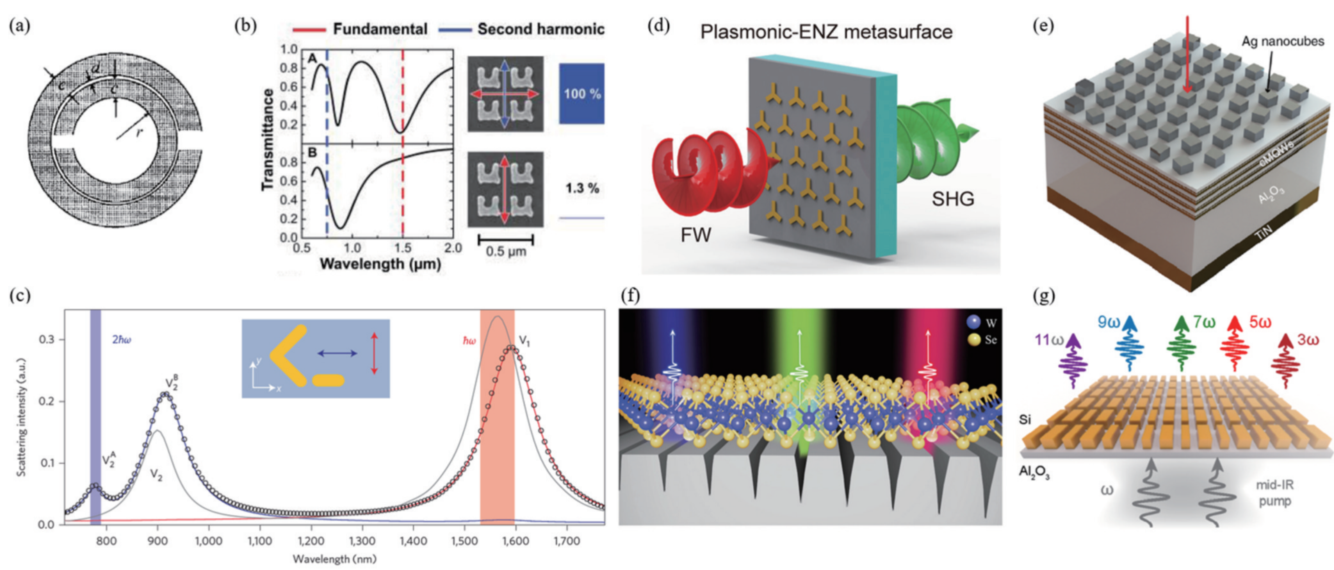

图2 非线性光学超构表面。(a)用于增强拉曼信号的磁共振超构材料[44]；(b)中心反演对称破缺U形超构单元上的倍频辐射[45]；(c)在基频和倍频波段具有双共振特性的超构单元[47]；(d)用于倍频产生的等离激元-ENZ复合超构表面[52]；(e)金属-量子阱复合非线性超构表面[54]；(f)金属-二维材料复合非线性超构表面[56]；(g)介质超构表面上的高次谐波产生[61]

Fig. 2 Nonlinear photonic metasurfaces. (a) Magnetic resonance metamaterial for Raman signal enhancement[44]; (b) second harmonic generation on central inversion symmetry broken U-shaped meta-atoms[45]; (c) meta-atoms with double resonance properties at fundamental and second harmonic frequencies[47]; (d) plasmonic-ENZ hybrid metasurface for second harmonic generation[52]; (e) metal-quantum well hybrid nonlinear metasurface[54]; (f) metal-two-dimensional material hybrid nonlinear metasurface[56]; (g) high harmonic generation from dielectric metasurface[61]

金属超构单元所具有的局域等离激元共振特性可在其邻近的非线性材料中产生强局域场，从而提高超构表面的非线性转化效率。以介电常数近零（ENZ）的氧化铟锡（ITO）为例，其二阶非线性极化率较强的张量元为$\chi_{zzz}^{(2)}$。当基频光正入射到ITO薄膜上时，薄膜中电场的z分量很小，产生的倍频信号较弱。若在ITO薄膜上制备金属超构单元使入射光的电场在ITO的ENZ波段被局域增强，则ITO薄膜中倍频光的产生效率会提升几个数量级[52]，如图2(d)所示。此外，图2(e)所示的金属-量子阱[53-55]、图2(f)所示的金属-二维材料[56]等复合体系也可以用于提高倍频光的转化效率。在可见-近红外波段中，金属-量子阱超构表面的倍频光转换效率可以达到10^{-4}[54]。

鉴于等离激元超构表面存在损耗高、共振品质因子低和损伤阈值低等问题，低损耗、高非线性极化率的介质材料[砷化镓（GaAs）、硅（Si）和锗（Ge）等]逐渐被用于新型非线性光学超构表面的设计中[42-43]。在介质超构表面上引入Fano共振[57]、图2(g)所示的连续谱中的束缚态（BIC）[58-61]和电磁诱导透明[62]等具有高品质因子的共振模式可以提高倍频、三倍频和高次谐波等非线性过程的转换效率。

3　非线性光学中的对称性和几何相位

3.1　对称性与非线性光学过程中的选择定则

晶体的对称性在非线性光学中扮演着重要的角色。一方面，晶体的对称性影响其线性极化率，进而决定了晶体的各向异性特性，相关理论被广泛应用于非线性过程中的相位匹配。另一方面，晶体的对称性会影响其非线性极化率的张量元。近年来，对称性选择的非线性过程被广泛用于超构表面研究领域中。在由各向同性材料组成的超构表面中，超构单元的对称性也会影响超构材料的非线性光学响应。例如，各向异性的超构单元在不同方向上具有不同的线性和非线性极化率。在倍频产生过程中，研究人员通常使用中心反演对称破缺的超构单元。对于关于y轴镜像对称的U形超构单元，其等效的二阶非线性极化率张量元满足$\chi_{yxx}^{(2)} \gg \chi_{yyy}^{(2)}$。因此，由U形超构单元组成的超构表面上的倍频光辐射呈现出明显的偏振选择性[45-46]。

近年来，手性超构材料因具备一些特殊的非线性光学响应而备受关注。手性光学材料通常具有旋光性（OA）和圆二向色性（CD）。传统材料的手性光学响应来源于其组成分子的手性，通常比较微弱[63-64]。设计强手性超构单元可以实现圆偏振光学器件和手性分子检测等功能[65-67]。在非线性光学过程中，研究人员发现手性超构表面上的四波混频、倍频和三倍频信号呈现出极强的CD[68-72]。如图3(a)所示，在具有三重和四重旋转对称性的手性超构单元上，引入面内的镜面对称性破缺可增强倍频光和三倍频光的CD[70]，实验中测得的倍频光CD和三倍频光CD分别高达98%和79%。这种面内镜像对称破缺一般不影响超构单元的线性光学特性，可以用于制备非线性光学“防伪水印”，只有通过非线性光学过程才能读出加密的图像[71]，如图3(b)所示。此外，在悬空的金/氮化硅薄膜上，通过聚焦离子束技术可以制备三维纳米剪纸超构表面，这类手性结构对不同圆偏振入射光的吸收有很大差异，实验中观测到了很强的倍频光CD[73]，如图3(c)所示。将手性等离激元超构表面与上转换纳米颗粒结合，利用手性分子对纳米颗粒上转换荧光的影响实现了灵敏的异构手性分子检测[74]，如图3(d)所示。

除此之外，旋转对称性也在非线性光学过程中起着重要的作用。在具有j重旋转对称性的非线性晶体或超构单元中，光子可以与晶体交换大小为$lj\hbar$（l为整

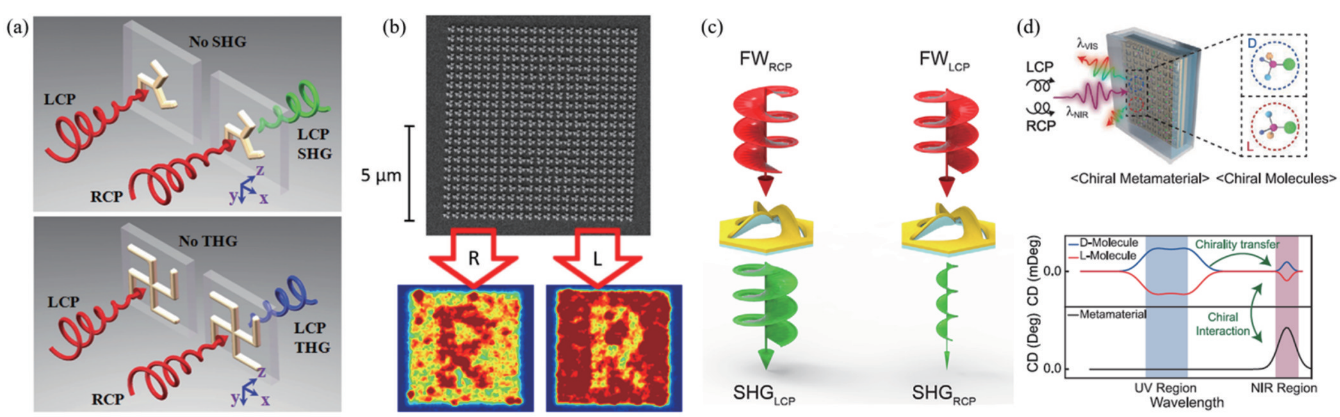

图3　手性非线性光学超构表面。(a)用于产生强CD倍频光和三倍频光的镜面对称破缺的C3和C4超构单元[70]；(b)超构表面与非线性手性“水印”[71]；(c)三维纳米剪纸超构表面上倍频光的强CD[73]；(d)基于上转换荧光技术的手性分子检测[74]

Fig. 3　Chiral nonlinear photonic metasurfaces. (a) Mirror symmetry broken C3 and C4 meta-atoms for second harmonic generation and third harmonic generation with strong CD [70]; (b) metasurface and nonlinear chiral "watermark"[71]; (c) strong CD of second harmonic generation from three-dimensional nano-kirigami metasurface[73]; (d) chiral molecule sensing based on up-conversion photoluminescence[74]

数)的角动量。当圆偏振光入射时,由于光与物质相互作用过程中角动量守恒,故允许产生的谐波级次为 $n=lj\pm1$[75-78]。通过设计制备具有特定旋转对称性的等离激元超构单元,在实验上验证了超构表面上倍频、三倍频、光整流和四波混频等非线性光学过程中的对称性选择定则[79-82]。

3.2 非线性光学过程中的几何相位

灵活的相位调控是实现对非线性光场进行复杂调控的基础。对于U形超构单元,通过翻转结构开口的方向可在其产生的倍频光场中引入0和π的相位调控[83],如图4(a)所示。这种二元相位的超构表面可以有效地对倍频光场的波前进行调控,实现光束偏折、聚焦等功能。然而,若要对非线性光场进行更复杂的调控,则需要对非线性光场进行0~2π的连续相位调控。根据线性光学范畴下的几何相位理论,在圆偏振入射光与各向异性的光学超构单元相互作用后,具有反向圆偏振分量的反射光或透射光会携带几何相位[84-92]。改变面内超构单元的朝向就可以在出射光场上引入与超构单元转角相关的几何相位 $\varphi=2\sigma\theta$,其中 θ 为超构单元的朝向角,$\sigma=\pm1$ 对应入射光的左旋圆偏振态或右旋圆偏振态。在偶极子近似条件下,非线性谐波辐射过程中也存在类似的几何相位[93-95],如图4(b)和图4(c)所示。对于一个 n 阶谐波过程,产生的同向和反向圆偏振谐波分别携带 $(n-1)\sigma\theta$ 和 $(n+1)\sigma\theta$ 的几何相位。对于1~5阶谐波产生过程,使用具有不同旋转对称性的超构单元,综合考虑对称性选择定则和非线性几何相位原理,可以得到谐波级次与几何相位之间的关系,如表2所示。其中,“+”表示谐波的圆偏振态与基频光相同,“−”表示谐波的圆偏振态与基频光相反,“×”表示该过程被对称性选择定则禁止。

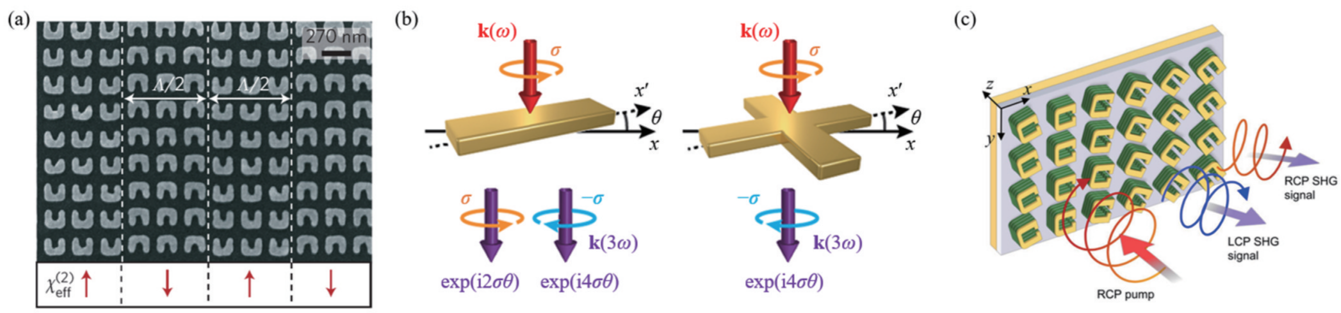

图4 非线性光学几何相位。(a) U形超构单元在倍频产生过程中引入0、π二元相位调控[83];(b) C2和C4超构单元产生的三倍频光所携带的几何相位[93];(c)利用U形超构单元实现对倍频光的几何相位调控[94]

Fig. 4 Nonlinear photonic geometric phase. (a) Binary phase control of 0 and π in second harmonic generation by U-shaped meta-atoms[83]; (b) geometric phases of third harmonic generation by C2 and C4 meta-atoms[93]; (c) geometric phase control of second harmonic generation by U-shaped meta-atoms[94]

表2 谐波产生过程中的几何相位

Table 2 Geometric phase in harmonic generation

Harmonic order	Sign of harmonic	C_1	C_2	C_3	C_4
$n=1$	+	×	×	×	×
	−	$2\theta\sigma$	$2\theta\sigma$	×	×
$n=2$	+	$\theta\sigma$	×	×	×
	−	$3\theta\sigma$	×	$3\theta\sigma$	×
$n=3$	+	$2\theta\sigma$	$2\theta\sigma$	×	×
	−	$4\theta\sigma$	$4\theta\sigma$	×	$4\theta\sigma$
$n=4$	+	$3\theta\sigma$	×	$3\theta\sigma$	×
	−	$5\theta\sigma$	×	×	×
$n=5$	+	$4\theta\sigma$	$4\theta\sigma$	×	$4\theta\sigma$
	−	$6\theta\sigma$	$6\theta\sigma$	$6\theta\sigma$	×

4 非线性光学超构表面的应用

4.1 基于非线性光学超构表面的波前调控器件

对每个超构单元所产生的非线性光场的相位和振幅进行控制可以实现复杂的波前调控功能。例如,改变硅超构单元的几何尺寸可以对其所产生的三倍频光进行0~2π的相位调控,从而实现非线性光束偏转、图5(a)所示的聚焦涡旋光束产生[96]和全息成像[97]等功能。在砷化镓超构表面上,通过和频过程可以将红外入射光参量上转换为可见光并成像,从而实现超薄的红外光成像器件[98]。基于非线性光学几何相位原理,改变具有三重旋转对称性的等离激元超构单元的朝向分布可实现超构表面上产生的倍频光的连续相位调控,从而实现聚焦、非线性成像[99]和图5(b)所示的轨道角动量光束产生等波前调控功能[100-101]。

若进一步考虑非线性光学超构表面的多极子或偏振响应,则可实现多通道信息加密功能。例如,在硅/氮化硅介质超构表面上,通过设计超构单元的米氏多极子共振响应可以控制其产生的前向和背向传播的三倍频信号强度,从而该超构表面在正向和背向入射的基频光泵浦下可以辐射出两幅不同的三倍频图像[102]。根据超构单元的偏振响应特性,可以设计对水平和竖直偏振的基频光响应的双层超构表面,最终可实现基于三倍频过程的偏振复用全息器件[103],如图5(c)所

示。根据线性和非线性几何相位原理，基频光和倍频光可携带与U形超构单元转角关系为$2\sigma\theta$、$\sigma\theta$和$3\sigma\theta$的线性与非线性几何相位，从而实现了频率-偏振复用的多通道全息成像器件[104]，如图5(d)所示。在左旋圆偏振和右旋圆偏振的基频光泵浦下，C3等离激元超构单元上产生的倍频光的非线性几何相位大小相等、方向相反。因此，当基频光为线偏振光时，所产生的倍频光也是线偏振的，并且其偏振方向由C3超构单元的朝向决定[79, 105]。根据这一原理，可以将灰度图像隐藏到倍频光的特定偏振分量中。该图像在普通可见光照明条件下不可见，只有正确地设置入射基频光和产生的倍频光的线偏振态后才能解密隐藏的灰度图像[105]，如图5(e)所示。此外，利用手性超构表面的非线性CD可以实现非线性图像加密[71]和全息成像[106]。

若将两个或多个超构单元组成一个新的“人工分子”，则可以利用相位型非线性超构单元实现对非线性信号的振幅调制[107]，如图5(f)所示。将两个C3超构单元上产生的倍频光进行相干叠加可以实现对倍频光的振幅和相位进行独立调控。根据这一原理，Mao等[108]将两幅图像分别储存于实空间和傅里叶空间中，如图5(g)所示。2022年，Mao等[109]设计了包含两组超构单元的四原子超构表面，并基于光场叠加原理和全息迭代算法，首次实现了非线性矢量全息成像，如图5(h)所示。

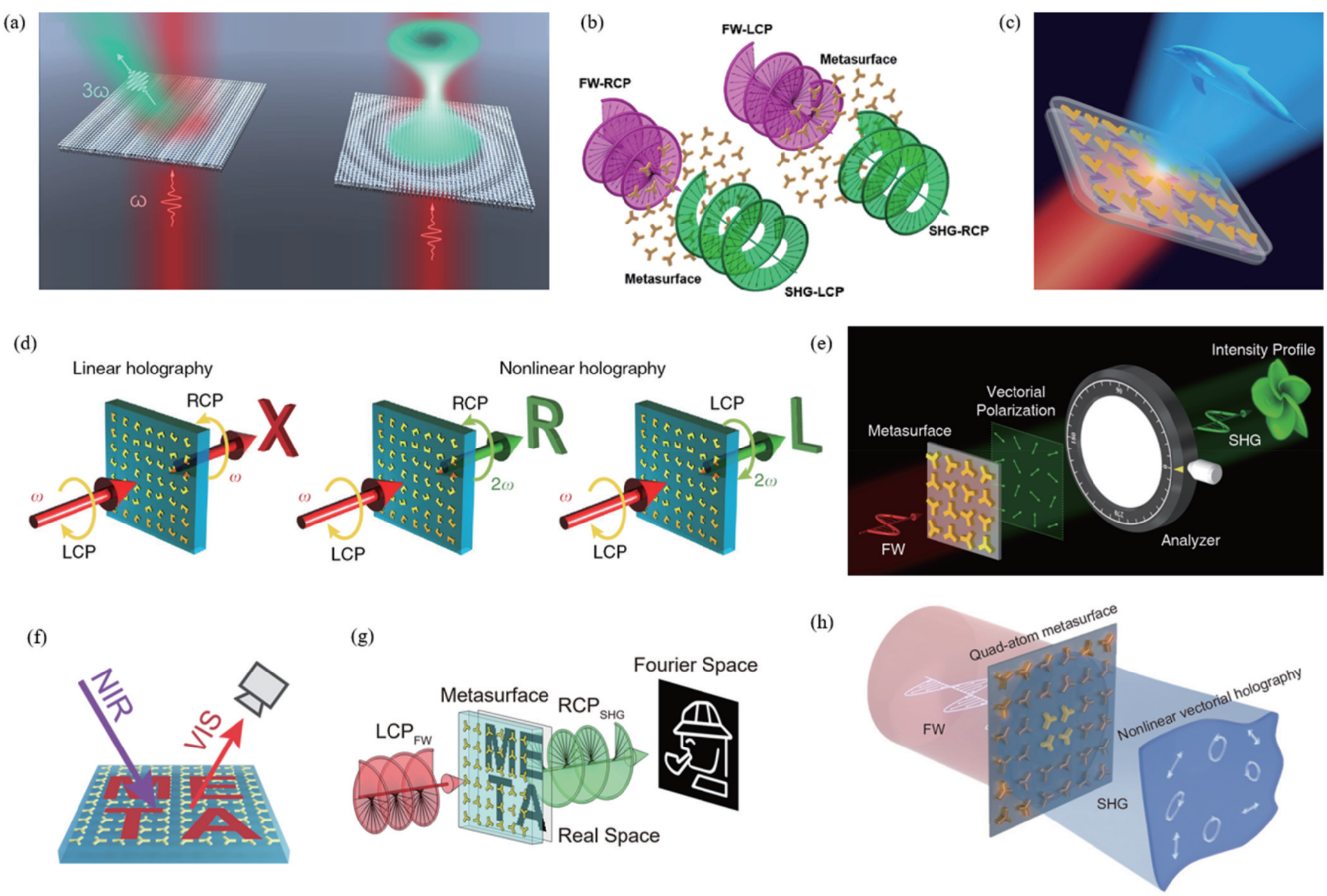

图5 非线性光学超构表面波前调控器件。(a)基于介质超构表面实现三倍频光束偏转和涡旋光束产生[96]；(b)等离激元超构表面上倍频光涡旋光束的产生[100]；(c)偏振复用三倍频全息成像[103]；(d)基于U形超构单元的频率-偏振复用多通道全息成像[104]；(e)基于C3超构单元的倍频光矢量光束产生和图像加密[105]；(f)用于倍频光图像加密的双原子非线性光学超构表面[107]；(g)基于双原子超构表面在实空间和傅里叶空间实现倍频光图像加密[108]；(h)基于四原子超构表面的非线性矢量全息成像[109]

Fig. 5 Nonlinear photonic metasurfaces for wavefront engineering. (a) Third harmonic generation beam steering and vortex beam generation based on dielectric metasurface[96]; (b) generation of second harmonic generation optical vortex on plasmonic metasurface[100]; (c) polarization-multiplexed third harmonic generation holography[103]; (d) frequency-polarization multiplexed multi-channel holography with U-shaped meta-atoms[104]; (e) second harmonic generation vectorial beam and image encoding based on C3 meta-atoms[105]; (f) diatomic nonlinear photonic metasurface for encryption of second harmonic generation image[107]; (g) diatomic metasurface for encryption of second harmonic generation image in both real and Fourier spaces[108]; (h) quad-atom metasurface for nonlinear vectorial holography[109]

4.2 非线性光学超构表面量子器件

在量子光学领域中，超构表面也展现出了重要的应用价值。例如，将超构表面与量子点结合可实现高效率和高亮度的单光子源[110-111]、圆偏振单光子源[112]和

携带轨道角动量的单光子源[113]。此外，超构表面也可以用来实现光子自旋与轨道角动量的纠缠[114]、光量子态的重建[115]、圆偏振 NOON 态[116]和量子干涉特性的调控[117-118]等。

1995 年，Kwiat 等[119]发现晶体中的参量下转换过程可产生高亮度的纠缠光子对，该方法已被广泛应用于量子光学领域的研究中。如图 6(a)所示，Liu 等[120]将环形布拉格谐振腔与量子点结合，产生了高亮度、不可分辨的偏振纠缠光子对。Ming 等[121]基于 U 形超构单元组成的非线性超构表面，提出了产生具有轨道角动量的纠缠双光子方法，如图 6(b)所示。Marino 等[122]通过设计铝砷化镓（AlGaAs）纳米柱的米氏共振使其同时在基频光子和下转换光子频率处共振，实现了高效率的双光子源，如图 6(c)所示。Santiago-Cruz 等[123]在砷化镓超构表面上，利用 BIC 产生了高品质因子的共振模式，并通过自发参量下转换过程产生了不同频率的纠缠光子对。如图 6(d)所示。此外，还可以通过将超构表面与非线性光学晶体级联的方法产生纠缠光子对。2020 年，Li 等[124]将 10×10 的超构透镜阵列与偏硼酸钡（β-BaB_2O_4，BBO）晶体结合，泵浦光经由 100 个超构透镜中的一个或多个聚焦至 BBO 晶体上，并通过自发参量下转换过程实现了多维双光子路径纠缠态，如图 6(e)所示。Zhang 等[125]在铌酸锂薄膜上制备了二氧化硅超构光栅，有效提高了产生纠缠光子对的效率，如图 6(f)所示。基于非线性光学超构表面对光子对自旋、频谱和空间等自由度的操控能力，科学家们还提出了时空量子超构表面的概念[126]。这些研究表明，超构表面在发展小型化纠缠量子光源并实现对光子的多自由度光场调控方面具有重要的应用价值[127-128]。

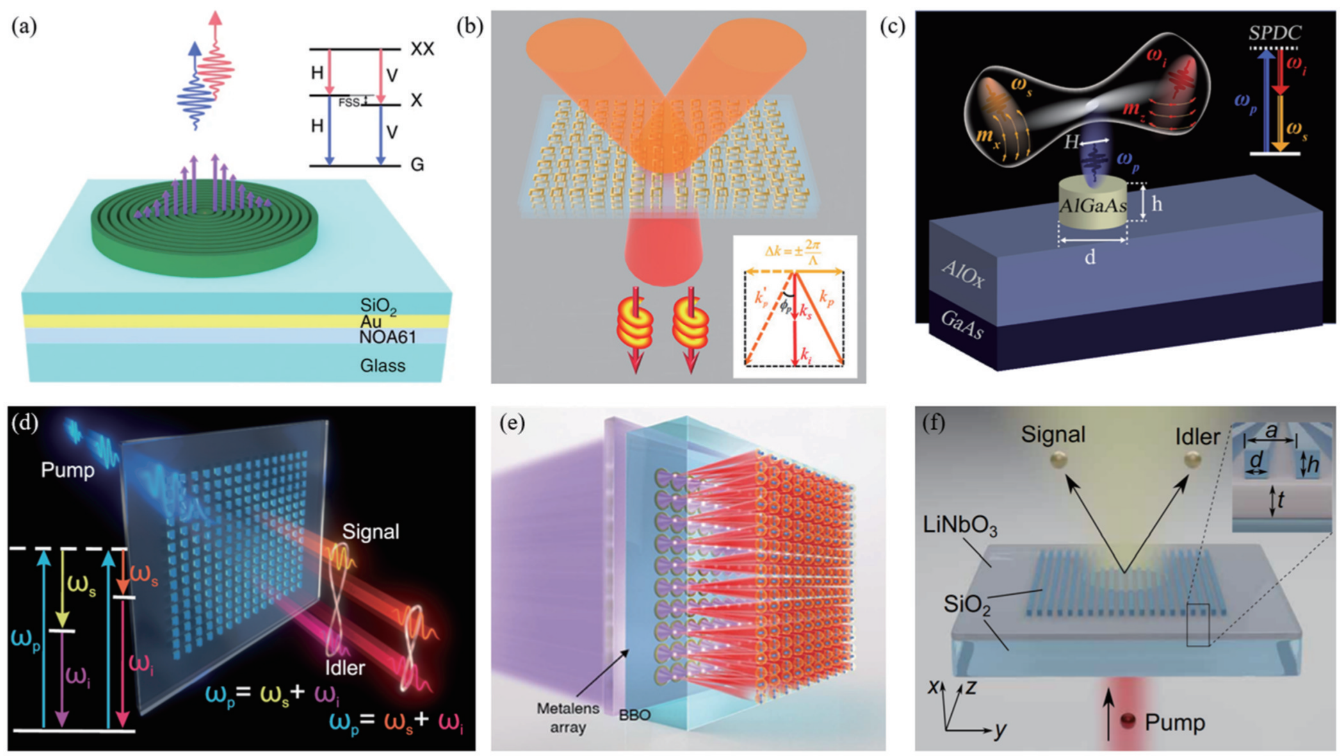

图 6　非线性光学超构表面与量子信息处理。(a)基于环形布拉格谐振腔与量子点的纠缠光源[120]；(b)非线性等离激元超构表面上产生携带轨道角动量的纠缠光子对[121]；(c)基于介质超构表面的双光子源[122]；(d)基于介质超构表面的多频率纠缠光源[123]；(e)利用超构透镜阵列和 BBO 晶体实现高维纠缠光源[124]；(f)基于 LN 薄膜与介质超构光栅的高效率纠缠光源[125]

Fig. 6　Nonlinear photonic metasurfaces for quantum information processing. (a) Circular Bragg resonator integrated with quantum dot for generating entangled photon pairs[120]; (b) nonlinear plasmonic metasurface for generating entangled photon pairs with orbital angular momentum[121]; (c) photon pair source based on dielectric metasurface[122]; (d) multi-frequency entangled source based on dielectric metasurface[123]; (e) high-dimensional entangled source realized by combining metalens array and BBO crystal[124]; (f) meta-gratings loaded LN thin film for generating entangled photon pairs with high efficiency[125]

4.3　太赫兹非线性超构表面

太赫兹波段的电磁波（0.1～10.0 THz，30 μm～3 mm）位于远红外和微波之间，因其具有的一些独特性质而引起了科研界和工业界的广泛关注。太赫兹波的光子能量低，故其能够穿透许多在可见光波段下不透明的材料，在非侵入和非电离式医学成像和诊断方面有着重要的应用前景。许多气体分子、有机材料和生物材料（蛋白质、细胞和脱氧核糖核酸等）的振动和转动能级间的跃迁通常发生在太赫兹频段，这促进了太赫兹光谱仪和太赫兹材料表征技术的发展。目前，

成熟的太赫兹波产生方法主要包括连续波量子级联激光技术[129]、光电导开关[130]、自由电子激光装置[131]和非线性晶体中的光整流效应[132]等。这些太赫兹辐射源能产生中等功率的连续或脉冲太赫兹波。在太赫兹波的光场调控方面，许多传统光学功能元件（偏振片、透镜和波片等）不再适用。虽然块状的塑料材料可用于制作透射式的太赫兹光学器件，但是材料的强吸收会显著降低器件的性能。近年来，超构表面逐渐被用于实现太赫兹波的偏振转化[133-134]、相位调制[135]、涡旋光束产生[136]和可编程操控[137]等功能。

与此同时，非线性光学超构表面也被用于太赫兹波的产生和同时调控。2014 年，Luo 等[138]利用金属 U 形超构单元的二阶非线性响应，通过光整流过程在等离激元超构表面上实现了宽带的太赫兹波产生，所得太赫兹波的振幅与毫米厚度的碲化锌（ZnTe）晶体上产生的太赫兹波相当。调控超构单元的排列和几何参数可以实现对所产生的太赫兹波的空间模式和偏振态等的调控。2019 年，Keren-Zur 等[139]通过翻转 U 形超构单元实现了对所产生的太赫兹波的 0、π 二元相位调制。将二元相位非线性太赫兹超构单元组成菲涅耳波带片，在近红外飞秒激光泵浦下可以将产生的不同频率的太赫兹波聚焦至不同位置[140]，如图 7(a)所示。近来，非线性几何相位理论也被用于设计非线性超构表面太赫兹源。基于具有 C3 旋转对称性的等离激元超构单元，McDonnell 等[81, 141]研究了太赫兹波产生的对称性选择定则，并实现了对太赫兹波的 0～2π 的连续相位调控，如图 7(b)所示。以该非线性超构表面太赫兹源为平台，科学家们首次观察到了太赫兹涡环脉冲[142]。此外，Lu 等[143]利用 U 形超构单元和非线性几何相位原理实现了梯度相位和螺旋相位超构表面太赫兹源，如图 7(c)所示。

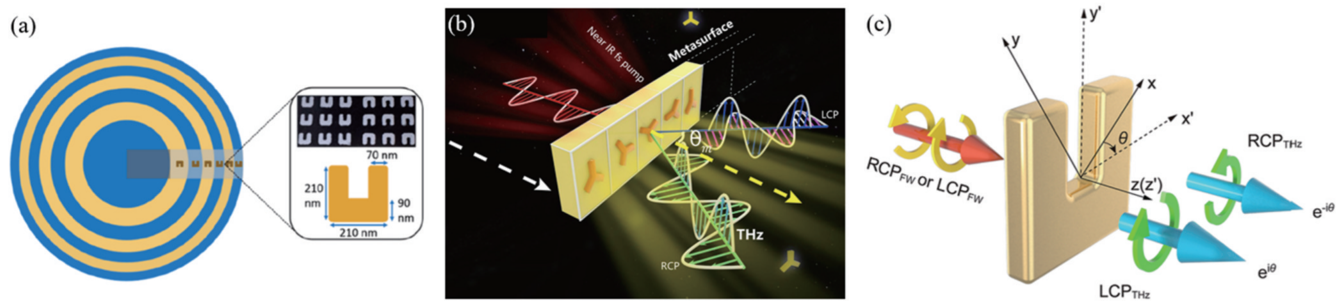

图 7 基于非线性超构表面的太赫兹辐射源。(a)等离激元超构表面上太赫兹波的产生与聚焦[140]；(b)基于金属 C3 超构单元的几何相位超构表面太赫兹源[81]；(c)基于 U 形超构单元的几何相位超构表面太赫兹源[143]

Fig. 7 Terahertz source based on nonlinear metasurface. (a) Plasmonic metasurface for terahertz generation and focusing[140]; (b) geometric phase metasurface terahertz source based on metallic C3 meta-atoms[81]; (c) geometric phase metasurface terahertz source based on U-shaped meta-atoms[143]

5 结束语

综述了非线性光学超构表面的基本原理与应用领域。首先，回顾了传统非线性光学中的相位匹配与准相位匹配技术，并介绍了基于铁电材料的非线性光子晶体的历史和最新进展。然后，基于等离激元与介质材料两种材料体系，讨论了非线性超构表面的发展历程，并总结了超构单元的对称性和几何相位原理在调控超构表面上非线性光场的偏振、相位等方面的重要作用。最后，介绍了一系列基于非线性光学超构表面的应用，如波前调控、图像加密、小型化量子纠缠光源和多功能太赫兹源等。

提高非线性光学超构表面的非线性转换效率是推进其实际应用的关键。在等离激元超构表面上，金属纳米结构在高泵浦功率下容易被欧姆损耗产生的热效应破坏，这阻碍了其转换效率的提升。介质超构表面具有损耗小、损伤阈值高的优点，工作在高泵浦功率下可以显著提高非线性光学转换效率。然而，利用介质超构表面来实现对非线性相位的调控对纳米结构的几何形状较为敏感，故加工制备过程具有较高的挑战性。基于非线性光学几何相位原理可以以非常简单的方式实现对非线性光场的相位调控，故该原理已在等离激元超构表面上取得了广泛应用，并有望推广至更多材料体系中。将线性超构表面与传统非线性晶体结合形成的复合器件能够兼顾晶体的高非线性转换效率和超构表面强大的光场调控能力[144]，相关领域的研究值得进一步探索。此外，借助新材料选择（如合成新晶体）或新的物理机制［如通过外加电场实现基于 $\chi^{(3)}$ 的电致倍频[145-146]］也有望提高倍频光的产生效率。

参 考 文 献

[1] 沈元壤. 非线性光学五十年[J]. 物理, 2012, 41(2): 71-81.
Shen Y R. 50 years of nonlinear optics[J]. Physics, 2012, 41(2): 71-81.

[2] Franken P A, Hill A E, Peters C W, et al. Generation of optical harmonics[J]. Physical Review Letters, 1961, 7(4): 118-119.

[3] 常国庆. Peter Franken 与非线性光学[J]. 物理, 2022, 51(7):

505-508.
Chang G Q. Peter Franken and nonlinear optics[J]. Physics, 2022, 51(7): 505-508.
[4] Shen Y R. The principles of nonlinear optics[M]. New York: John Wiley & Sons, 1984.
[5] Boyd R W. Nonlinear optics [M]. 4th ed. London: Academic Press, 2020.
[6] Armstrong J A, Bloembergen N, Ducuing J, et al. Interactions between light waves in a nonlinear dielectric[J]. Physical Review, 1962, 127(6): 1918-1939.
[7] Giordmaine J A. Mixing of light beams in crystals[J]. Physical Review Letters, 1962, 8(1): 19-20.
[8] Maker P D, Terhune R W, Nisenoff M, et al. Effects of dispersion and focusing on the production of optical harmonics [J]. Physical Review Letters, 1962, 8(1): 21-22.
[9] Midwinter J E, Warner J. The effects of phase matching method and of uniaxial crystal symmetry on the polar distribution of second-order non-linear optical polarization[J]. British Journal of Applied Physics, 1965, 16(8): 1135-1142.
[10] Fejer M M, Magel G A, Jundt D H, et al. Quasi-phase-matched second harmonic generation: tuning and tolerances[J]. IEEE Journal of Quantum Electronics, 1992, 28(11): 2631-2654.
[11] Feng D, Ming N B, Hong J F, et al. Enhancement of second-harmonic generation in $LiNbO_3$ crystals with periodic laminar ferroelectric domains[J]. Applied Physics Letters, 1980, 37(7): 607-609.
[12] Yamada M, Nada N, Saitoh M, et al. First-order quasi-phase matched $LiNbO_3$ waveguide periodically poled by applying an external field for efficient blue second-harmonic generation[J]. Applied Physics Letters, 1993, 62(5): 435-436.
[13] Zhu S N, Zhu Y Y, Qin Y Q, et al. Experimental realization of second harmonic generation in a Fibonacci optical superlattice of $LiTaO_3$[J]. Physical Review Letters, 1997, 78(14): 2752-2755.
[14] Zhu S N, Zhu Y Y, Ming N B. Quasi-phase-matched third-harmonic generation in a quasi-periodic optical superlattice[J]. Science, 1997, 278(5339): 843-846.
[15] Chen B Q, Ren M L, Liu R J, et al. Simultaneous broadband generation of second and third harmonics from chirped nonlinear photonic crystals[J]. Light: Science & Applications, 2014, 3(7): e189.
[16] Hong L H, Chen B Q, Hu C Y, et al. Ultrabroadband nonlinear Raman-Nath diffraction against femtosecond pulse laser[J]. Photonics Research, 2022, 10(4): 905-912.
[17] Berger V. Nonlinear photonic crystals[J]. Physical Review Letters, 1998, 81(19): 4136-4139.
[18] Chen J J, Chen X F. Phase matching in three-dimensional nonlinear photonic crystals[J]. Physical Review A, 2009, 80(1): 013801.
[19] Wei D Z, Wang C W, Wang H J, et al. Experimental demonstration of a three-dimensional lithium niobate nonlinear photonic crystal[J]. Nature Photonics, 2018, 12(10): 596-600.
[20] Xu T X, Switkowski K, Chen X, et al. Three-dimensional nonlinear photonic crystal in ferroelectric barium calcium titanate [J]. Nature Photonics, 2018, 12(10): 591-595.
[21] Liu S, Switkowski K, Xu C L, et al. Nonlinear wavefront shaping with optically induced three-dimensional nonlinear photonic crystals[J]. Nature Communications, 2019, 10: 3208.
[22] Wei D Z, Wang C W, Xu X Y, et al. Efficient nonlinear beam shaping in three-dimensional lithium niobate nonlinear photonic crystals[J]. Nature Communications, 2019, 10: 4193.
[23] Xu X Y, Wang T X, Chen P C, et al. Femtosecond laser writing of lithium niobate ferroelectric nanodomains[J]. Nature, 2022, 609(7927): 496-501.
[24] Keren-Zur S, Ellenbogen T. A new dimension for nonlinear photonic crystals[J]. Nature Photonics, 2018, 12(10): 575-577.
[25] Zhang Y, Sheng Y, Zhu S N, et al. Nonlinear photonic crystals: from 2D to 3D[J]. Optica, 2021, 8(3): 372-381.
[26] Veselago V G. The electrodynamics of substances with simultaneously negative values of ε and μ[J]. Soviet Physics Uspekhi, 1968, 10(4): 509-514.
[27] Shelby R A, Smith D R, Schultz S. Experimental verification of a negative index of refraction[J]. Science, 2001, 292(5514): 77-79.
[28] Soukoulis C M, Wegener M. Optical metamaterials: more bulky and less lossy[J]. Science, 2010, 330(6011): 1633-1634.
[29] Soukoulis C M, Wegener M. Past achievements and future challenges in the development of three-dimensional photonic metamaterials[J]. Nature Photonics, 2011, 5(9): 523-530.
[30] Zheludev N I, Kivshar Y S. From metamaterials to metadevices [J]. Nature Materials, 2012, 11(11): 917-924.
[31] Cai W S, Shalaev V M. Optical metamaterials: fundamentals and applications[M]. New York: Springer, 2010.
[32] Yu N F, Genevet P, Kats M A, et al. Light propagation with phase discontinuities: generalized laws of reflection and refraction [J]. Science, 2011, 334(6054): 333-337.
[33] Kildishev A V, Boltasseva A, Shalaev V M. Planar photonics with metasurfaces[J]. Science, 2013, 339(6125): 1232009.
[34] Glybovski S B, Tretyakov S A, Belov P A, et al. Metasurfaces: from microwaves to visible[J]. Physics Reports, 2016, 634: 1-72.
[35] Chen H T, Taylor A J, Yu N F. A review of metasurfaces: physics and applications[J]. Reports on Progress in Physics, 2016, 79(7): 076401.
[36] Hu J, Bandyopadhyay S, Liu Y H, et al. A review on metasurface: from principle to smart metadevices[J]. Frontiers in Physics, 2021, 8: 586087.
[37] Kim J, Seong J, Yang Y, et al. Tunable metasurfaces towards versatile metalenses and metaholograms: a review[J]. Advanced Photonics, 2022, 4(2): 024001.
[38] Zhou H Q, Li X, Xu Z T, et al. Correlated triple hybrid amplitude and phase holographic encryption based on a metasurface[J]. Photonics Research, 2022, 10(3): 678-686.
[39] Minovich A E, Miroshnichenko A E, Bykov A Y, et al. Functional and nonlinear optical metasurfaces[J]. Laser & Photonics Reviews, 2015, 9(2): 195-213.
[40] Li G X, Zhang S, Zentgraf T. Nonlinear photonic metasurfaces [J]. Nature Reviews Materials, 2017, 2: 17010.
[41] Krasnok A, Tymchenko M, Alù A. Nonlinear metasurfaces: a paradigm shift in nonlinear optics[J]. Materials Today, 2018, 21(1): 8-21.
[42] Kivshar Y. All-dielectric meta-optics and non-linear nanophotonics[J]. National Science Review, 2018, 5(2): 144-158.
[43] Sain B, Meier C, Zentgraf T. Nonlinear optics in all-dielectric nanoantennas and metasurfaces: a review[J]. Advanced Photonics, 2019, 1(2): 024002.
[44] Pendry J B, Holden A J, Robbins D J, et al. Magnetism from conductors and enhanced nonlinear phenomena[J]. IEEE Transactions on Microwave Theory and Techniques, 1999, 47(11): 2075-2084.
[45] Klein M W, Enkrich C, Wegener M, et al. Second-harmonic generation from magnetic metamaterials[J]. Science, 2006, 313(5786): 502-504.
[46] Zhang X C, Deng J H, Jin M K, et al. Giant enhancement of second-harmonic generation from a nanocavity metasurface[J]. Science China Physics, Mechanics & Astronomy, 2021, 64(9): 294215.
[47] Celebrano M, Wu X F, Baselli M, et al. Mode matching in multiresonant plasmonic nanoantennas for enhanced second harmonic generation[J]. Nature Nanotechnology, 2015, 10(5): 412-417.
[48] Niesler F P, Niesler F B P, Forstner J, et al. Collective effects in second-harmonic generation from split-ring-resonator arrays

[J]. Physical Review Letters, 2012, 109(1): 015502.
[49] Czaplicki R, Kiviniemi A, Laukkanen J, et al. Surface lattice resonances in second-harmonic generation from metasurfaces[J]. Optics Letters, 2016, 41(12): 2684-2687.
[50] Michaeli L, Keren-Zur S, Avayu O, et al. Nonlinear surface lattice resonance in plasmonic nanoparticle arrays[J]. Physical Review Letters, 2017, 118(24): 243904.
[51] Czaplicki R, Husu H N, Siikanen R, et al. Enhancement of second-harmonic generation from metal nanoparticles by passive elements[J]. Physical Review Letters, 2013, 110(9): 093902.
[52] Deng J H, Tang Y T, Chen S M, et al. Giant enhancement of second-order nonlinearity of epsilon-near- zero medium by a plasmonic metasurface[J]. Nano Letters, 2020, 20(7): 5421-5427.
[53] Lee J, Tymchenko M, Argyropoulos C, et al. Giant nonlinear response from plasmonic metasurfaces coupled to intersubband transitions[J]. Nature, 2014, 511(7507): 65-69.
[54] Qian H L, Li S L, Chen C F, et al. Large optical nonlinearity enabled by coupled metallic quantum wells[J]. Light: Science & Applications, 2019, 8: 13.
[55] Sarma R, de Ceglia D, Nookala N, et al. Broadband and efficient second-harmonic generation from a hybrid dielectric metasurface/semiconductor quantum-well structure[J]. ACS Photonics, 2019, 6(6): 1458-1465.
[56] Ding Y F, Wei C R, Su H M, et al. Second harmonic generation covering the entire visible range from a 2D material-plasmon hybrid metasurface[J]. Advanced Optical Materials, 2021, 9(16): 2100625.
[57] Yang Y M, Wang W Y, Boulesbaa A, et al. Nonlinear Fano-resonant dielectric metasurfaces[J]. Nano Letters, 2015, 15(11): 7388-7393.
[58] Carletti L, Koshelev K, de Angelis C, et al. Giant nonlinear response at the nanoscale driven by bound states in the continuum [J]. Physical Review Letters, 2018, 121(3): 033903.
[59] Koshelev K, Tang Y T, Li K, et al. Nonlinear metasurfaces governed by bound states in the continuum[J]. ACS Photonics, 2019, 6(7): 1639-1644.
[60] Koshelev K, Kruk S, Melik-Gaykazyan E, et al. Subwavelength dielectric resonators for nonlinear nanophotonics [J]. Science, 2020, 367(6475): 288-292.
[61] Zograf G, Koshelev K, Zalogina A, et al. High-harmonic generation from resonant dielectric metasurfaces empowered by bound states in the continuum[J]. ACS Photonics, 2022, 9(2): 567-574.
[62] Liu H Z, Guo C, Vampa G, et al. Enhanced high-harmonic generation from an all-dielectric metasurface[J]. Nature Physics, 2018, 14(10): 1006-1010.
[63] Hazen R M, Sholl D S. Chiral selection on inorganic crystalline surfaces[J]. Nature Materials, 2003, 2(6): 367-374.
[64] Ernst K H. Molecular chirality at surfaces[J]. Physica Status Solidi (b), 2012, 249(11): 2057-2088.
[65] Hentschel M, Schäferling M, Duan X Y, et al. Chiral plasmonics[J]. Science Advances, 2017, 3(5): e1602735.
[66] Mun J, Kim M, Yang Y, et al. Electromagnetic chirality: from fundamentals to nontraditional chiroptical phenomena[J]. Light, Science & Applications, 2020, 9: 139.
[67] Chen Y, Du W, Zhang Q, et al. Multidimensional nanoscopic chiroptics[J]. Nature Reviews Physics, 2022, 4(2): 113-124.
[68] Rose A, Powell D A, Shadrivov I V, et al. Circular dichroism of four-wave mixing in nonlinear metamaterials[J]. Physical Review B, 2013, 88(19): 195148.
[69] Rodrigues S P, Lan S F, Kang L, et al. Nonlinear imaging and spectroscopy of chiral metamaterials[J]. Advanced Materials, 2014, 26(35): 6157-6162.
[70] Chen S M, Zeuner F, Weismann M, et al. Giant nonlinear optical activity of achiral origin in planar metasurfaces with quadratic and cubic nonlinearities[J]. Advanced Materials, 2016, 28(15): 2992-2999.
[71] Kolkowski R, Petti L, Rippa M, et al. Octupolar plasmonic meta-molecules for nonlinear chiral watermarking at subwavelength scale[J]. ACS Photonics, 2015, 2(7): 899-906.
[72] Frizyuk K, Melik-Gaykazyan E, Choi J H, et al. Nonlinear circular dichroism in Mie-resonant nanoparticle dimers[J]. Nano Letters, 2021, 21(10): 4381-4387.
[73] Tang Y T, Liu Z G, Deng J H, et al. Nano-Kirigami metasurface with giant nonlinear optical circular dichroism[J]. Laser & Photonics Reviews, 2020, 14(7): 2000085.
[74] Lee K T, Kim B, Raju L, et al. Enantiomer-selective molecular sensing in the nonlinear optical regime via upconverting chiral metamaterials[J]. Advanced Functional Materials, 2022, 32(43): 2208641.
[75] Simon H J, Bloembergen N. Second-harmonic light generation in crystals with natural optical activity[J]. Physical Review, 1968, 171(3): 1104-1114.
[76] Burns W K, Bloembergen N. Third-harmonic generation in absorbing media of cubic or isotropic symmetry[J]. Physical Review B, 1971, 4(10): 3437-3450.
[77] Tang C L, Rabin H. Selection rules for circularly polarized waves in nonlinear optics[J]. Physical Review B, 1971, 3(12): 4025-4034.
[78] Saito N, Xia P Y, Lu F M, et al. Observation of selection rules for circularly polarized fields in high-harmonic generation from a crystalline solid[J]. Optica, 2017, 4(11): 1333-1336.
[79] Konishi K, Higuchi T, Li J, et al. Polarization-controlled circular second-harmonic generation from metal hole arrays with threefold rotational symmetry[J]. Physical Review Letters, 2014, 112(13): 135502.
[80] Chen S M, Li G X, Zeuner F, et al. Symmetry-selective third-harmonic generation from plasmonic metacrystals[J]. Physical Review Letters, 2014, 113(3): 033901.
[81] McDonnell C, Deng J H, Sideris S, et al. Functional THz emitters based on Pancharatnam-Berry phase nonlinear metasurfaces[J]. Nature Communications, 2021, 12(1): 30.
[82] Li G X, Sartorello G, Chen S M, et al. Spin and geometric phase control four-wave mixing from metasurfaces[J]. Laser & Photonics Reviews, 2018, 12(6): 1800034.
[83] Segal N, Keren-Zur S, Hendler N, et al. Controlling light with metamaterial-based nonlinear photonic crystals[J]. Nature Photonics, 2015, 9(3): 180-184.
[84] Berry M V. Quantal phase factors accompanying adiabatic changes[J]. Proceedings of the Royal Society of London A, 1984, 392(1802): 45-57.
[85] Berry M V. The adiabatic phase and Pancharatnam's phase for polarized light[J]. Journal of Modern Optics, 1987, 34(11): 1401-1407.
[86] Pancharatnam S. Generalized theory of interference and its applications[J]. Proceedings of the Indian Academy of Sciences-Section A, 1956, 44(6): 398-417.
[87] Tomita A, Chiao R Y. Observation of Berry's topological phase by use of an optical fiber[J]. Physical Review Letters, 1986, 57(8): 937-940.
[88] Haldane F D. Path dependence of the geometric rotation of polarization in optical fibers[J]. Optics Letters, 1986, 11(11): 730-732.
[89] Bomzon Z, Biener G, Kleiner V, et al. Space-variant Pancharatnam-Berry phase optical elements with computer-generated subwavelength gratings[J]. Optics Letters, 2002, 27(13): 1141-1143.
[90] Cohen E, Larocque H, Bouchard F, et al. Geometric phase from Aharonov-Bohm to Pancharatnam-Berry and beyond[J]. Nature Reviews Physics, 2019, 1(7): 437-449.
[91] Xie X, Pu M B, Jin J J, et al. Generalized Pancharatnam-Berry phase in rotationally symmetric meta-atoms[J]. Physical Review Letters, 2021, 126(18): 183902.

[92] Cisowski C M, Götte J B, Franke-Arnold S. *Colloquium*: geometric phases of light: insights from fiber bundle theory[J]. Reviews of Modern Physics, 2022, 94(3): 031001.

[93] Li G X, Chen S M, Pholchai N, et al. Continuous control of the nonlinearity phase for harmonic generations[J]. Nature Materials, 2015, 14(6): 607-612.

[94] Tymchenko M, Gomez-Diaz J S, Lee J, et al. Gradient nonlinear Pancharatnam-Berry metasurfaces[J]. Physical Review Letters, 2015, 115(20): 207403.

[95] Karnieli A, Li Y Y, Arie A. The geometric phase in nonlinear frequency conversion[J]. Frontiers of Physics, 2022, 17(1): 12301.

[96] Wang L, Kruk S, Koshelev K, et al. Nonlinear wavefront control with all-dielectric metasurfaces[J]. Nano Letters, 2018, 18(6): 3978-3984.

[97] Gao Y S, Fan Y B, Wang Y J, et al. Nonlinear holographic all-dielectric metasurfaces[J]. Nano Letters, 2018, 18(12): 8054-8061.

[98] del Rocio Camacho-Morales M, Rocco D, Xu L, et al. Infrared upconversion imaging in nonlinear metasurfaces[J]. Advanced Photonics, 2021, 3(3): 036002.

[99] Schlickriede C, Waterman N, Reineke B, et al. Imaging through nonlinear metalens using second harmonic generation[J]. Advanced Materials, 2018, 30(8): 1703843.

[100] Li G X, Wu L, Li K F, et al. Nonlinear metasurface for simultaneous control of spin and orbital angular momentum in second harmonic generation[J]. Nano Letters, 2017, 17(12): 7974-7979.

[101] Chen S M, Li K, Deng J H, et al. High-order nonlinear spin-orbit interaction on plasmonic metasurfaces[J]. Nano Letters, 2020, 20(12): 8549-8555.

[102] Kruk S S, Wang L, Sain B, et al. Asymmetric parametric generation of images with nonlinear dielectric metasurfaces[J]. Nature Photonics, 2022, 16(8): 561-565.

[103] Almeida E, Bitton O, Prior Y. Nonlinear metamaterials for holography[J]. Nature Communications, 2016, 7: 12533.

[104] Ye W M, Zeuner F, Li X, et al. Spin and wavelength multiplexed nonlinear metasurface holography[J]. Nature Communications, 2016, 7: 11930.

[105] Tang Y T, Intaravanne Y, Deng J H, et al. Nonlinear vectorial metasurface for optical encryption[J]. Physical Review Applied, 2019, 12(2): 024028.

[106] Wang M J, Li Y, Tang Y T, et al. Nonlinear chiroptical holography with Pancharatnam-Berry phase controlled plasmonic metasurface[J]. Laser & Photonics Reviews, 2022, 16(12): 2200350.

[107] Walter F, Li G X, Meier C, et al. Ultrathin nonlinear metasurface for optical image encoding[J]. Nano Letters, 2017, 17(5): 3171-3175.

[108] Mao N B, Deng J H, Zhang X C, et al. Nonlinear diatomic metasurface for real and Fourier space image encoding[J]. Nano Letters, 2020, 20(10): 7463-7468.

[109] Mao N B, Zhang G Q, Tang Y T, et al. Nonlinear vectorial holography with quad-atom metasurfaces[J]. Proceedings of the National Academy of Sciences of the United States of America, 2022, 119(22): e2204418119.

[110] Wang H, He Y M, Chung T H, et al. Towards optimal single-photon sources from polarized microcavities[J]. Nature Photonics, 2019, 13(11): 770-775.

[111] Vaskin A, Kolkowski R, Koenderink A F, et al. Light-emitting metasurfaces[J]. Nanophotonics, 2019, 8(7): 1151-1198.

[112] Kan Y H, Andersen S K H, Ding F, et al. Metasurface-enabled generation of circularly polarized single photons[J]. Advanced Materials, 2020, 32(16): e1907832.

[113] Chen B, Wei Y M, Zhao T M, et al. Bright solid-state sources for single photons with orbital angular momentum[J]. Nature Nanotechnology, 2021, 16(3): 302-307.

[114] Stav T, Faerman A, Maguid E, et al. Quantum entanglement of the spin and orbital angular momentum of photons using metamaterials[J]. Science, 2018, 361(6407): 1101-1104.

[115] Wang K, Titchener J G, Kruk S S, et al. Quantum metasurface for multiphoton interference and state reconstruction[J]. Science, 2018, 361(6407): 1104-1108.

[116] Georgi P, Massaro M, Luo K H, et al. Metasurface interferometry toward quantum sensors[J]. Light: Science & Applications, 2019, 8: 70.

[117] Jha P K, Ni X J, Wu C, et al. Metasurface-enabled remote quantum interference[J]. Physical Review Letters, 2015, 115(2): 025501.

[118] Li Q W, Bao W, Nie Z Y, et al. A non-unitary metasurface enables continuous control of quantum photon-photon interactions from bosonic to fermionic[J]. Nature Photonics, 2021, 15(4): 267-271.

[119] Kwiat P G, Mattle K, Weinfurter H, et al. New high-intensity source of polarization-entangled photon pairs[J]. Physical Review Letters, 1995, 75(24): 4337-4341.

[120] Liu J, Su R B, Wei Y M, et al. A solid-state source of strongly entangled photon pairs with high brightness and indistinguishability[J]. Nature Nanotechnology, 2019, 14(6): 586-593.

[121] Ming Y, Zhang W, Tang J, et al. Photonic entanglement based on nonlinear metamaterials[J]. Laser & Photonics Reviews, 2020, 14(5): 1900146.

[122] Marino G, Solntsev A S, Xu L, et al. Spontaneous photon-pair generation from a dielectric nanoantenna[J]. Optica, 2019, 6(11): 1416-1422.

[123] Santiago-Cruz T, Gennaro S D, Mitrofanov O, et al. Resonant metasurfaces for generating complex quantum states[J]. Science, 2022, 377(6609): 991-995.

[124] Li L, Liu Z X, Ren X F, et al. Metalens-array-based high-dimensional and multiphoton quantum source[J]. Science, 2020, 368(6498): 1487-1490.

[125] Zhang J H, Ma J Y, Parry M, et al. Spatially entangled photon pairs from lithium niobate nonlocal metasurfaces[J]. Science Advances, 2022, 8(30): eabq4240.

[126] Kort-Kamp W J M, Azad A K, Dalvit D A R. Space-time quantum metasurfaces[J]. Physical Review Letters, 2021, 127(4): 043603.

[127] Solntsev A S, Agarwal G S, Kivshar Y S. Metasurfaces for quantum photonics[J]. Nature Photonics, 2021, 15(5): 327-336.

[128] 李林, 程亚, 祝世宁. 浅谈超构表面在量子光学中的应用[J]. 物理, 2021, 50(5): 308-316.
Li L, Cheng Y, Zhu S N. Metasurface-based quantum optics[J]. Physics, 2021, 50(5): 308-316.

[129] Song H J, Ajito K, Wakatsuki A, et al. Terahertz wireless communication link at 300 GHz[C]//2010 IEEE International Topical Meeting on Microwave Photonics, October 5-9, 2010, Montreal, QC, Canada. New York: IEEE Press, 2010: 42-45.

[130] Burford N M, El-Shenawee M O. Review of terahertz photoconductive antenna technology[J]. Optical Engineering, 2017, 56(1): 010901.

[131] Tan P, Huang J, Liu K F, et al. Terahertz radiation sources based on free electron lasers and their applications[J]. Science China Information Sciences, 2012, 55(1): 1-15.

[132] Yeh K L, Hoffmann M C, Hebling J, et al. Generation of 10 μJ ultrashort terahertz pulses by optical rectification[J]. Applied Physics Letters, 2007, 90(17): 171121.

[133] Grady N K, Heyes J E, Chowdhury D R, et al. Terahertz metamaterials for linear polarization conversion and anomalous refraction[J]. Science, 2013, 340(6138): 1304-1307.

[134] Jia M, Wang Z, Li H T, et al. Efficient manipulations of circularly polarized terahertz waves with transmissive metasurfaces[J]. Light: Science & Applications, 2019, 8: 16.

[135] Li J S, Yao J Q. Manipulation of terahertz wave using coding

Pancharatnam-Berry phase metasurface[J]. IEEE Photonics Journal, 2018, 10(5): 5900512.

[136] 李晓楠, 周璐, 赵国忠. 基于反射超表面产生太赫兹涡旋波束[J]. 物理学报, 2019, 68(23): 238101.
Li X N, Zhou L, Zhao G Z. Terahertz vortex beam generation based on reflective metasurface[J]. Acta Physica Sinica, 2019, 68(23): 238101.

[137] Tian H W, Shen H Y, Zhang X G, et al. Terahertz metasurfaces: toward multifunctional and programmable wave manipulation[J]. Frontiers in Physics, 2020, 8: 584077.

[138] Luo L, Chatzakis I, Wang J G, et al. Broadband terahertz generation from metamaterials[J]. Nature Communications, 2014, 5: 3055.

[139] Keren-Zur S, Tal M, Fleischer S, et al. Generation of spatiotemporally tailored terahertz wavepackets by nonlinear metasurfaces[J]. Nature Communications, 2019, 10(1): 1778.

[140] Minerbi E, Keren-Zur S, Ellenbogen T. Nonlinear metasurface Fresnel zone plates for terahertz generation and manipulation[J]. Nano Letters, 2019, 19(9): 6072-6077.

[141] McDonnell C, Deng J H, Sideris S, et al. Terahertz metagrating emitters with beam steering and full linear polarization control[J]. Nano Letters, 2022, 22(7): 2603-2610.

[142] Zdagkas A, McDonnell C, Deng J H, et al. Observation of toroidal pulses of light[J]. Nature Photonics, 2022, 16(7): 523-528.

[143] Lu Y C, Feng X, Wang Q W, et al. Integrated terahertz generator-manipulators using epsilon-near-zero-hybrid nonlinear metasurfaces[J]. Nano Letters, 2021, 21(18): 7699-7707.

[144] Mao N B, Tang Y T, Jin M K, et al. Nonlinear wavefront engineering with metasurface decorated quartz crystal[J]. Nanophotonics, 2022, 11(4): 797-803.

[145] Timurdogan E, Poulton C V, Byrd M J, et al. Electric field-induced second-order nonlinear optical effects in silicon waveguides[J]. Nature Photonics, 2017, 11(3): 200-206.

[146] Chen S M, Li K F, Li G X, et al. Gigantic electric-field-induced second harmonic generation from an organic conjugated polymer enhanced by a band-edge effect[J]. Light: Science & Applications, 2019, 8: 17.

Nonlinear Photonic Metasurfaces: Fundamentals and Applications

Tang Yutao, Zhang Xuecai, Hu Zixian, Hu Yue, Liu Xuan, Li Guixin*

Department of Materials Science and Engineering, College of Engineering, Southern University of Science and Technology, Shenzhen 518055, *Guangdong, China*

Abstract

Significance Optical metasurfaces are quasi-two-dimensional artificial materials that consist of subwavelength-scale meta-atoms. Thanks to the ultrathin footprints and versatile design degrees of freedom, a variety of metasurfaces have been designed and implemented to achieve novel optical devices or applications such as metalenses, meta-holograms, polarizers, waveplates, spin-to-orbit angular momentum converters, image encryption and polarimeters. By choosing the material constituents and geometries of the meta-atoms, one can easily manipulate the degrees of freedom of light fields, such as amplitude, polarization, phase, and frequency. The ability to exploit frequency as an additional channel relies on nonlinear optical processes, which involve the generation of nonlinear waves at new frequencies. Previous studies in nonlinear optics mainly focus on improving the conversion efficiencies of nonlinear processes, and the manipulation of the generated nonlinear waves is usually realized by linear optical elements. One of the most prominent advantages of nonlinear photonic metasurfaces is their capability to manipulate nonlinear waves while generating them, and therefore people can greatly shrink the devices into a more compact form.

The phase matching condition is of critical importance in traditional nonlinear optical processes based on photonic crystals (Table 1). The quasi-phase matching technique is proposed to improve conversion efficiency when the rigorous phase matching condition is not met (Fig. 1). Nonlinear photonic crystals are a class of artificially engineered structures that can be modulated spatially. They are capable of fulfilling the phase matching condition and realizing nonlinear wavefront shaping simultaneously. As for metasurfaces, because of the subwavelength-scale feature size, the phase matching condition is less rigorous than that in conventional nonlinear crystals. There are many materials and mechanisms that can be chosen to enhance nonlinear responses and to enrich the functionalities of nonlinear photonic metasurfaces (Fig. 2). With the rapid development of nonlinear metasurfaces in recent years, it is time to review the progress in the area. This paper discusses the fundamentals of the effects of symmetries and geometric phases on the nonlinear responses of the metasurfaces and the applications in nonlinear wavefront shaping, quantum information processing, and terahertz wave generation and manipulation based on nonlinear metasurfaces.

Progress The important roles of symmetries and geometric phases in nonlinear photonic metasurfaces are first discussed. While the symmetries of the meta-atoms can decide the allowed and forbidden nonlinear processes, they can also affect the chiral optical responses of the metasurfaces (Fig. 3). The nonlinear geometric phase is dependent on the order of the harmonic generations, the circular polarizations of the fundamental and nonlinear waves, and the spatial orientations of the meta-atoms (Fig. 4). It provides a convenient route to continuously control the phase imparted into the nonlinear waves (Table 2), which underpins the multi-dimensional nonlinear wavefront shaping by metasurfaces.

The applications based on nonlinear metasurfaces are then discussed. The direct applications of nonlinear metasurfaces are wavefront shaping devices (Fig. 5). With the ability to control the phases in nonlinear optical processes such as second harmonic generation, third harmonic generation, sum frequency generation, difference frequency generation, and four-wave mixing, the nonlinear metasurfaces have enabled nonlinear wavefront shaping like focusing, imaging, beam steering, vortex beam generation, holography, and image encryption. By exploiting the quantum entanglement characteristics of spontaneous down conversion processes, one can also use metasurfaces to generate high-dimensional entangled photons (Fig. 6). Several applications such as high-dimensional spatially entangled photon pairs and orbital angular momentum-carrying entangled photon pairs based on plasmonic and dielectric metasurfaces have been experimentally demonstrated. The nonlinear metasurfaces can be used for terahertz wave generation and manipulation as well. Terahertz waves possess unique advantages in applications such as nondestructive measurements and communications, but the development of terahertz technology is impeded by the lack of terahertz sources, detectors, and elements. Nonlinear metasurfaces represent a novel platform for simultaneously generating and manipulating terahertz waves. The concept of geometric phase has been successfully applied to the terahertz wave generation process (Fig. 7), which may lead to more functional devices in the terahertz spectral region.

Conclusions and Prospects To push forward the practical applications of nonlinear photonic metasurfaces, the key issue is to improve nonlinear conversion efficiency. All-dielectric metasurfaces can avoid the thermal heating effect that leads to the breakdown of the nanostructures in plasmonic metasurfaces and operate at a high pumping intensity to achieve high conversion efficiency. However, the nonlinear phase control ability of dielectric metasurfaces is very sensitive to the geometries of the nanostructures, which poses challenges to nanofabrication. The nonlinear geometric phases demonstrated on plasmonic metasurfaces provide an elegant way to manipulate the phase of nonlinear optical waves, which may be applied to more material systems. Moreover, the hybrid system of linear metasurfaces combined with traditional nonlinear crystals can provide a route to achieve highly efficient nonlinear wavefront engineering. Novel materials like new crystals or physical mechanisms such as electric field-induced second harmonic generation may also be exploited to improve the efficiency of second harmonic generation.

Key words optical design; nonlinear optics; photonic metasurfaces; wavefront engineering